Supplementary Information for

Vegetation greening and its environmental drivers across glacier forefields of the Third Pole

Qian Cheng[a,b], Xiaodan Wang[a,*], Zhengrong Yuan[a]

[a] Institute of Mountain Hazards and Environment, Chinese Academy of Sciences, Chengdu 610041, China;

[b] University of Chinese Academy of Sciences, Beijing 100049, China

[*] Corresponding author.

E-mail address: wxd@imde.ac.cn (X. Wang)

Table S1. Definitions of the temperature and precipitation extreme indices listed in this supplement.

Index	Index name	Definition	Unit
Temperature extreme indices			
TN10p	Cool nights	Percentage of days in a year with daily minimum temperature below the 10th-percentile threshold.	% days
TX10p	Cool days	Percentage of days in a year with daily maximum temperature below the 10th-percentile threshold.	% days
TN90p	Warm nights	Percentage of days in a year with daily minimum temperature above the 90th-percentile threshold.	% days
TX90p	Warm days	Percentage of days in a year with daily maximum temperature above the 90th-percentile threshold.	% days
DTR	Diurnal temperature range	Annual mean of the difference between daily maximum and minimum temperatures.	°C
TNn	Minimum daily minimum temperature	Lowest daily minimum temperature in a year.	°C
TXx	Maximum daily maximum temperature	Highest daily maximum temperature in a year.	°C
FD	Frost days	Number of days in a year with daily minimum temperature below 0 °C.	days
ID	Icing days	Number of days in a year with daily maximum temperature below 0 °C.	days
Precipitation extreme indices			
Rx1day	Maximum 1-day precipitation	Maximum daily precipitation in a year.	mm
Rx5day	Maximum consecutive 5-day precipitation	Maximum precipitation total over five consecutive days in a year.	mm
R95pTOT	Precipitation on very wet days	Annual total precipitation on days with precipitation exceeding the 95th-percentile threshold.	mm
R99pTOT	Precipitation on extremely wet days	Annual total precipitation on days with precipitation exceeding the 99th-percentile threshold.	mm
R10mm	Heavy precipitation days	Number of days in a year with daily precipitation ≥ 10 mm.	days
R20mm	Very heavy precipitation days	Number of days in a year with daily precipitation ≥ 20 mm.	days
CWD	Consecutive wet days	Maximum number of consecutive days in a year with daily precipitation ≥ 1 mm.	days
SDII	Simple daily intensity index	Annual total precipitation on wet days divided by the number of wet days.	mm day^{-1}

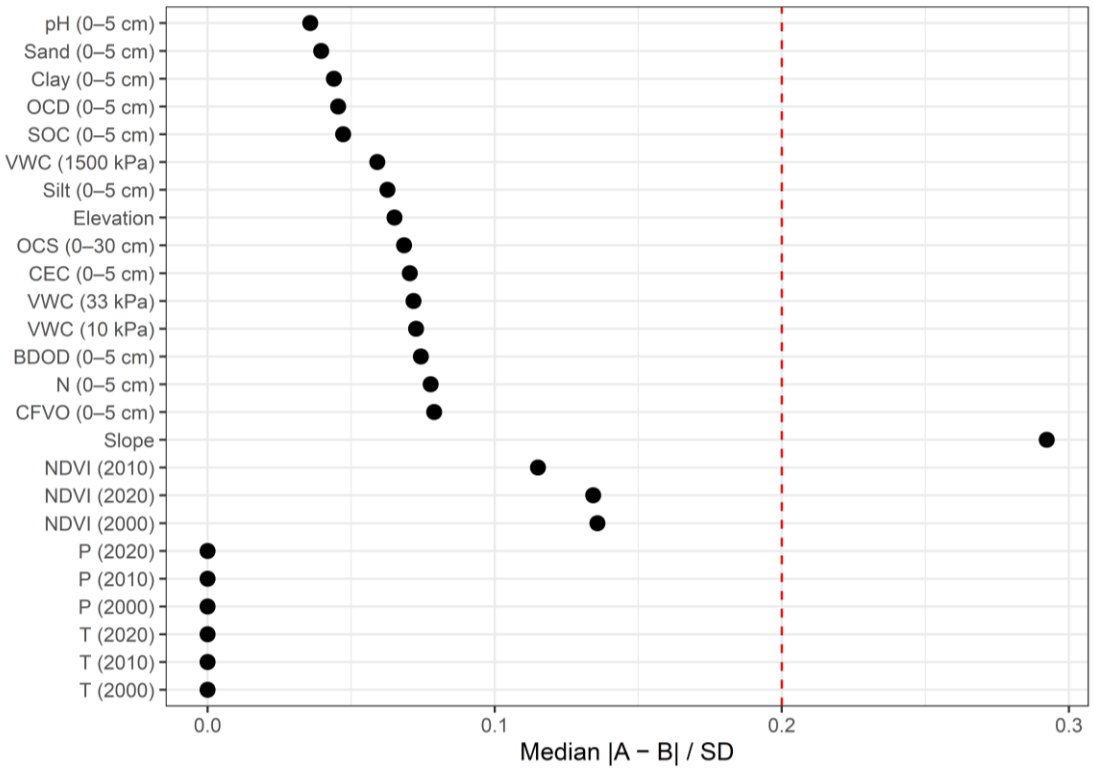


Figure S1. Standardized differences in environmental and vegetation variables between two independent random samples. Points show the median standardized absolute difference for each variable, calculated as Median |A − B| / SD. The red dashed line indicates a reference threshold of 0.2.

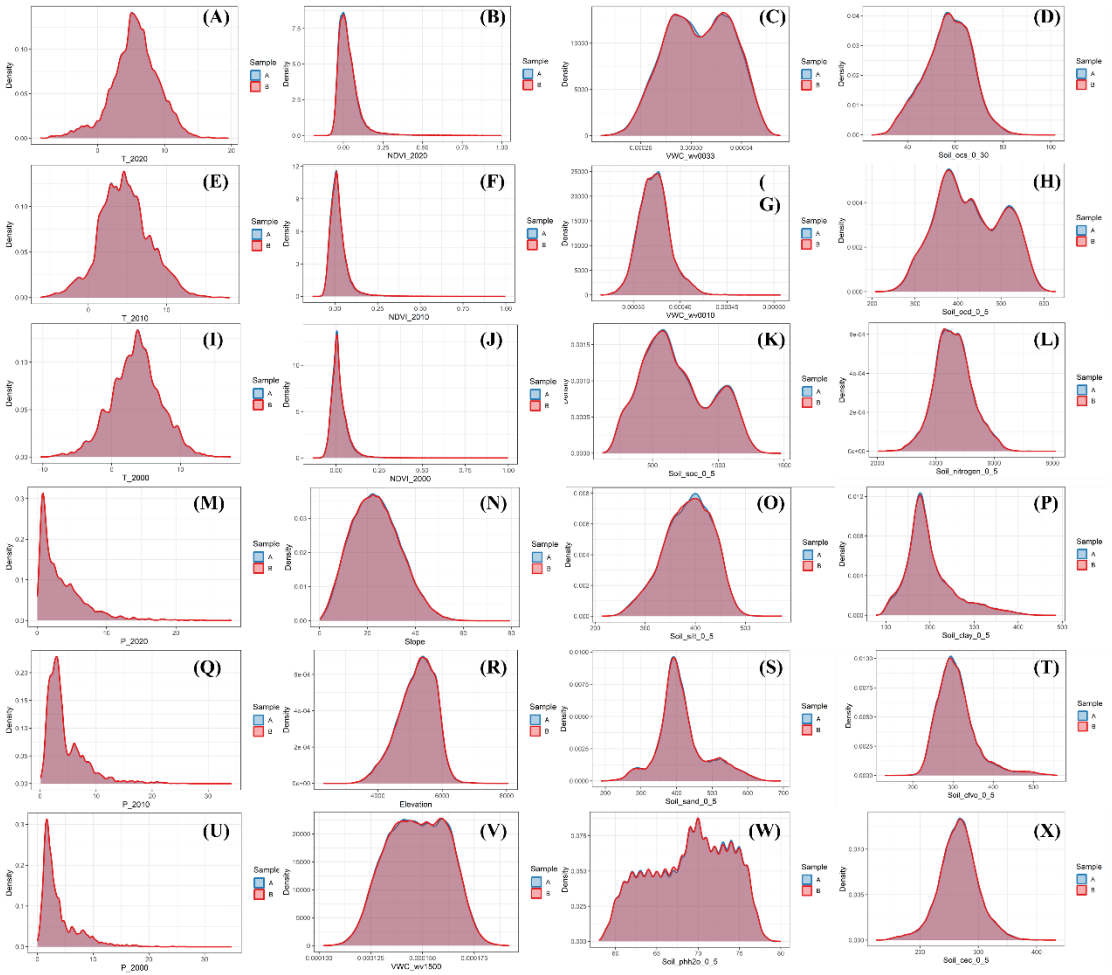


Figure S2. Comparison of kernel density distributions of environmental and vegetation variables between two independent random samples. Panels show distributions of temperature (T_2000, T_2010 and T_2020), precipitation (P_2000, P_2010 and P_2020), and the normalized difference vegetation index (NDVI_2000, NDVI_2010 and NDVI_2020). They also show topographic variables (slope and elevation) and soil properties, including volumetric water content, soil organic carbon (SOC), nitrogen, sand, silt, clay, pH and cation exchange capacity (CEC).

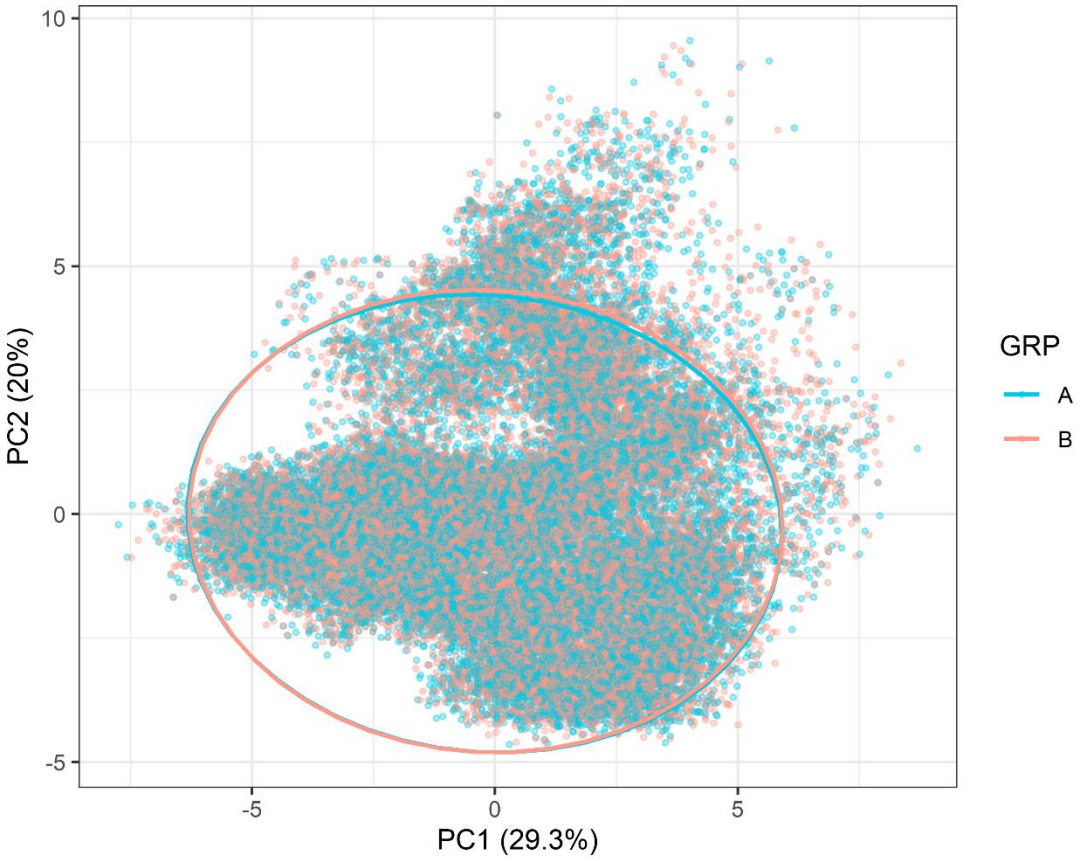


Figure S3. Comparison of two independent random samples in principal component analysis (PCA) space. Each point represents an individual sample projected onto the first two principal components. Ellipses summarize the spread of the two sample groups.

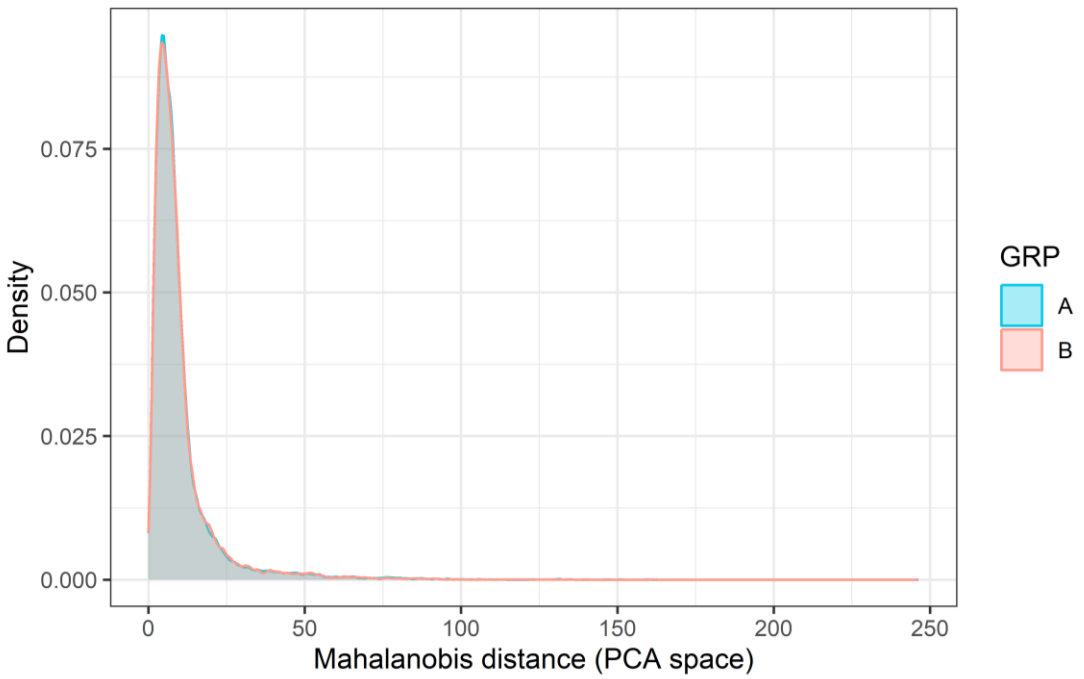


Figure S4. Distributions of Mahalanobis distances from two independent random samples to the centroid of sample set A in PCA space.

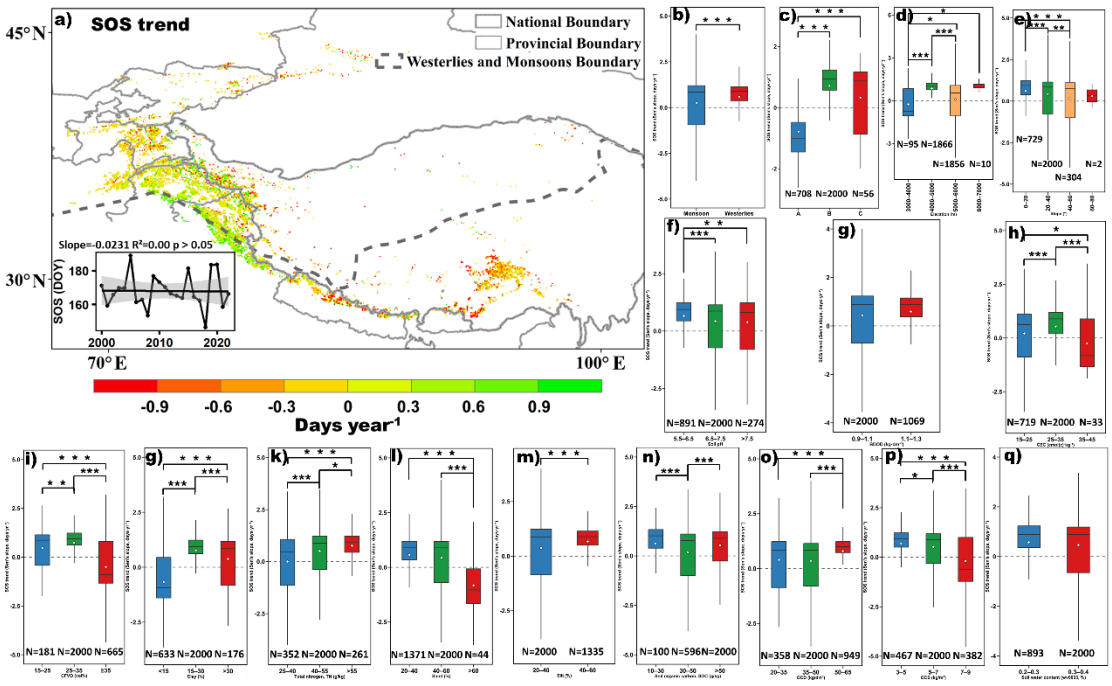


Figure S5. Trends in the start of the growing season (SOS) across glacier forefields of the Third Pole.

(a) Spatial pattern of SOS trends during 2000–2022. (b) Comparison between the monsoon and westerly regions. (c) Comparison among deglaciation-age groups (group A, glacier retreat before 1990; group B, retreat during 1990–2006; and group C, retreat after 2006). (d) Variation among elevation bands. (e) Variation among slope classes. (f–q) Variation among categories of soil properties. Boxes span the interquartile range, horizontal lines indicate medians, and points indicate means. The gray dashed line marks a trend slope of zero. Asterisks indicate statistical significance: *p < 0.05, **p < 0.01 and ***p < 0.001.

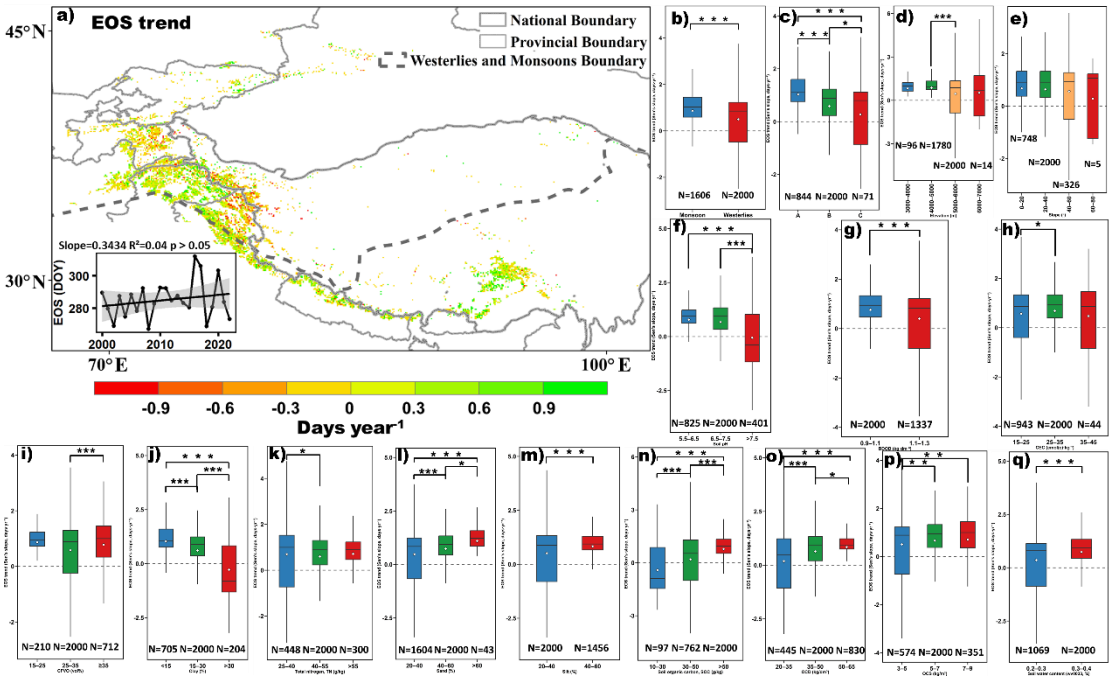


Figure S6. Trends in the end of the growing season (EOS) across glacier forefields of the Third Pole.

(a) Spatial pattern of EOS trends during 2000–2022. (b) Comparison between the monsoon and westerly regions. (c) Comparison among deglaciation-age groups (group A, glacier retreat before 1990; group B, retreat during 1990–2006; and group C, retreat after 2006). (d) Variation among elevation bands. (e) Variation among slope classes. (f–q) Variation among categories of soil properties. Boxes span the interquartile range, horizontal lines indicate medians, and points indicate means. The gray dashed line marks a trend slope of zero. Asterisks indicate statistical significance: *p < 0.05, **p < 0.01 and ***p < 0.001.

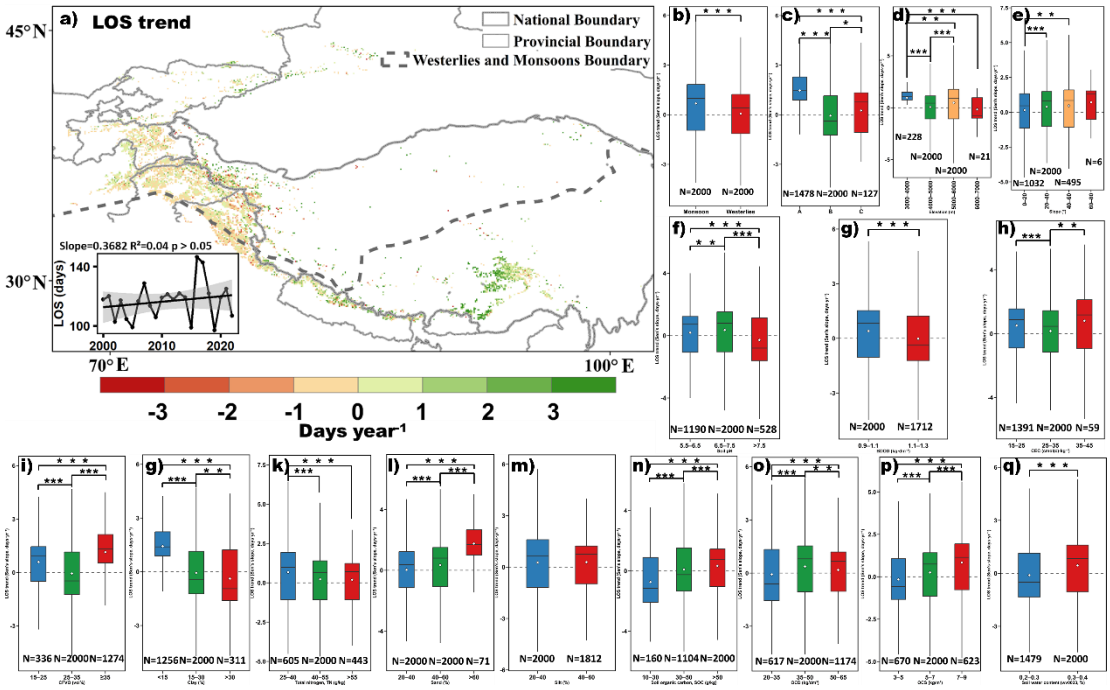


Figure S7. Trends in the length of the growing season (LOS) across glacier forefields of the Third Pole.

(a) Spatial pattern of LOS trends during 2000–2022. (b) Comparison between the monsoon and westerly regions. (c) Comparison among deglaciation-age groups (group A, glacier retreat before 1990; group B, retreat during 1990–2006; and group C, retreat after 2006). (d) Variation among elevation bands. (e) Variation among slope classes. (f–q) Variation among categories of soil properties. Boxes span the interquartile range, horizontal lines indicate medians, and points indicate means. The gray dashed line marks a trend slope of zero. Asterisks indicate statistical significance: *p < 0.05, **p < 0.01 and ***p < 0.001.

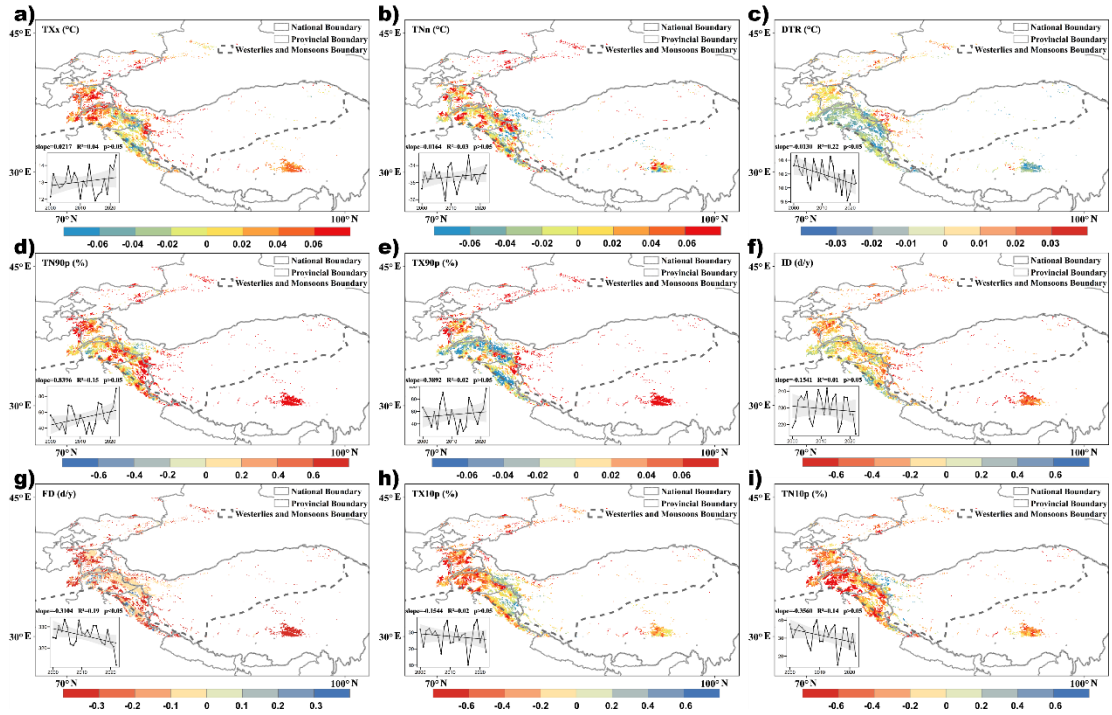


Figure S8. Spatial patterns of trends in temperature extreme indices across glacier forefields of the Third Pole.

(a–i) Spatial patterns of trends in nine temperature extreme indices during 2000–2022. Panels show (a) TXx, annual maximum daily maximum temperature; (b) TNn, annual minimum daily minimum temperature; (c) DTR, diurnal temperature range; (d) TN90p, warm-night frequency; (e) TX90p, warm-day frequency; (f) ID, icing days; (g) FD, frost days; (h) TX10p, cool-day frequency; and (i) TN10p, cool-night frequency. Colors indicate the trend slope at each sampling point, with the direction and magnitude specified by the color bar in each panel. Insets in the lower left show interannual variation in the regional mean of each index and its linear trend. Gray dashed lines mark the boundary between the westerly and monsoon regions.

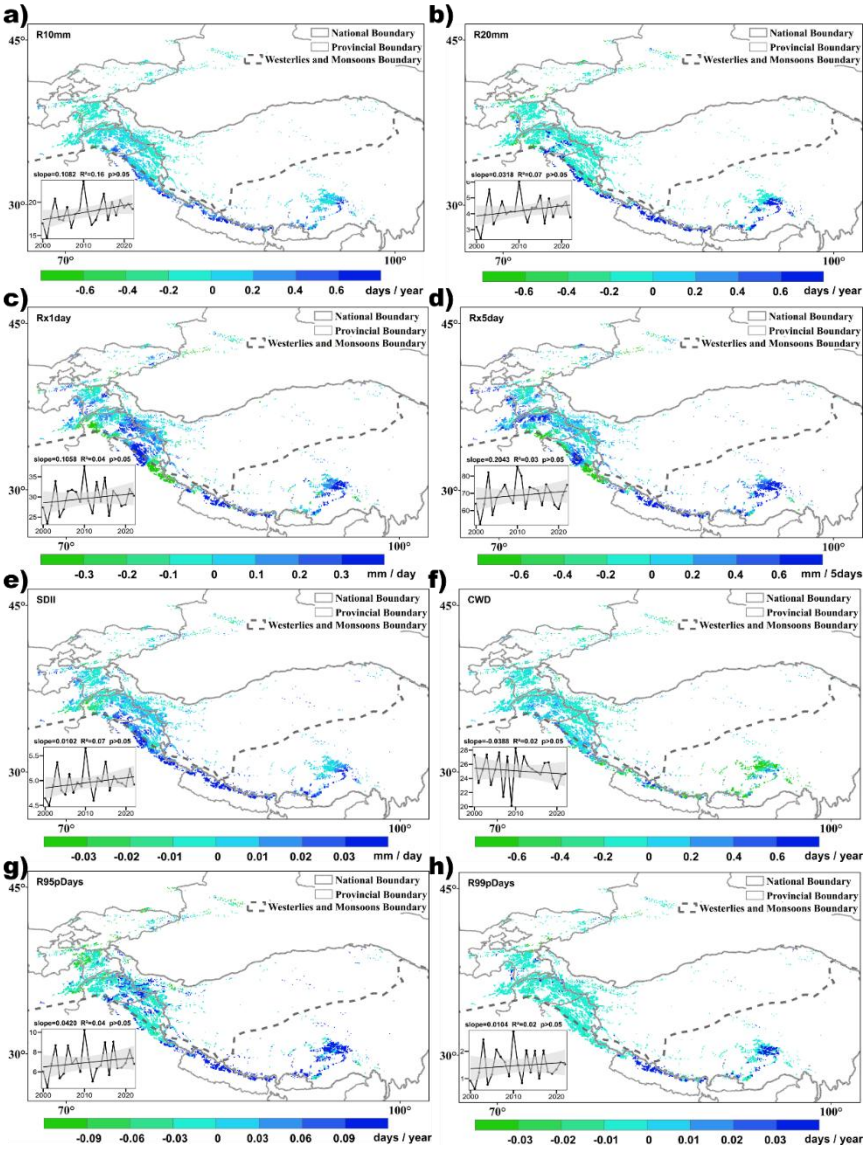


Figure S9. Spatial patterns of trends in precipitation extreme indices across glacier forefields of the Third Pole.

(a–h) Spatial patterns of trends in eight precipitation extreme indices during 2000–2022. Panels show (a) R10mm, heavy precipitation days; (b) R20mm, very heavy precipitation days; (c) Rx1day, annual maximum 1-day precipitation; (d) Rx5day, annual maximum consecutive 5-day precipitation; (e) SDII, simple daily intensity index; (f) CWD, consecutive wet days; (g) R95pDays, very wet days; and (h) R99pDays, extremely wet days. Colors indicate the trend slope at each sampling point, with green indicating decreasing trends and blue indicating increasing trends. Insets in the lower left show interannual variation in the regional mean of each index and its linear trend. Gray dashed lines mark the boundary between the westerly and monsoon regions.

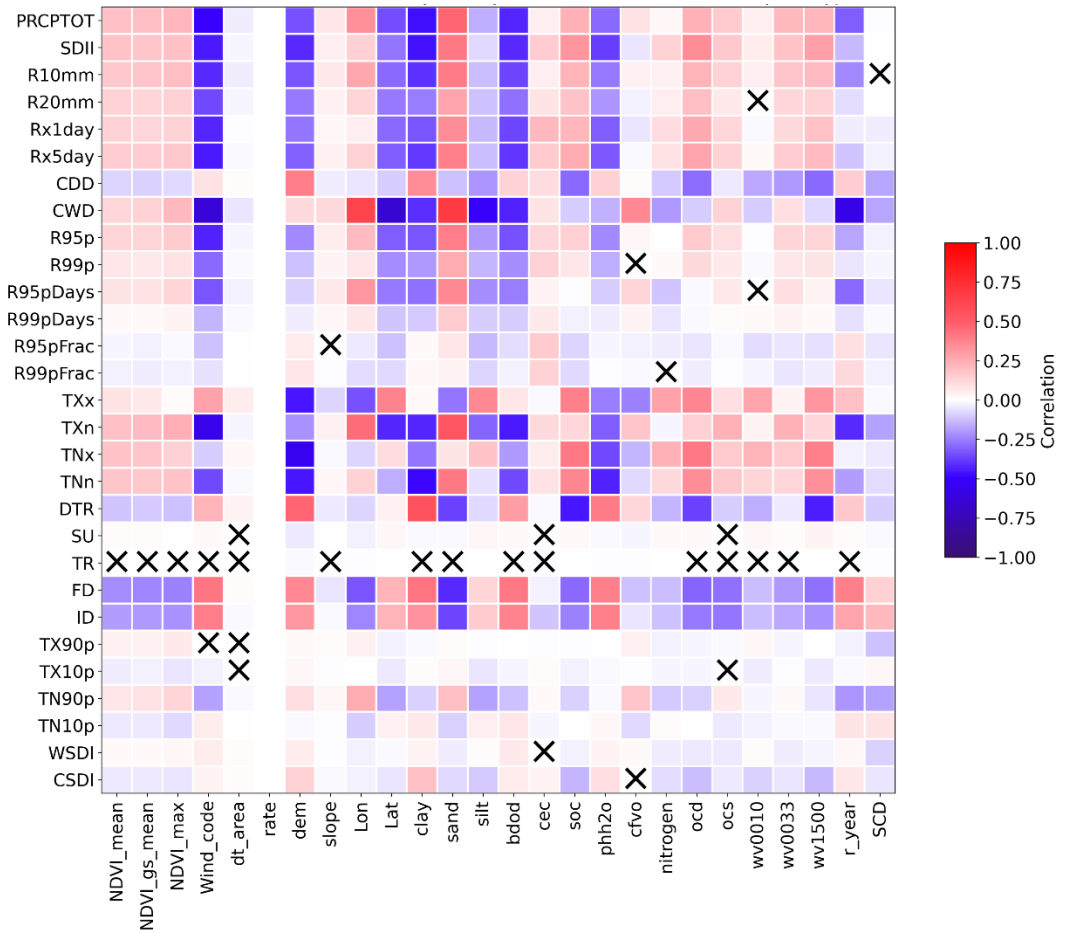


Figure S10. Correlations between extreme climate indices and NDVI, wind and other environmental variables in glacier forefields.

Rows represent extreme climate indices, and columns represent NDVI, wind and other environmental variables. Colors indicate correlation coefficients, with red denoting positive correlations and blue denoting negative correlations; greater color intensity indicates stronger correlations. Crosses (×) mark correlations that are not statistically significant ($p \geq 0.05$).

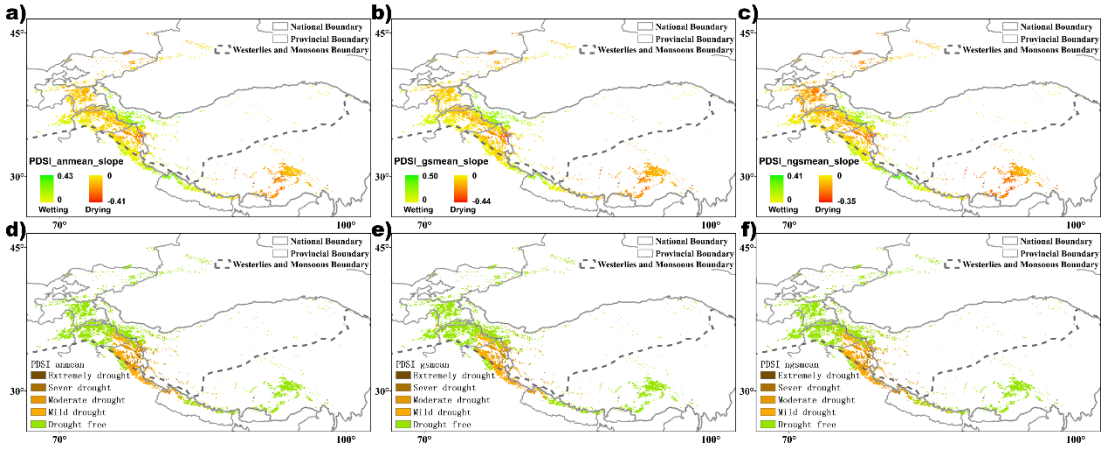


Figure S11. Spatial patterns of trends in the Palmer Drought Severity Index (PDSI) and PDSI-based drought categories across glacier forefields of the Third Pole.

(a–c) Spatial patterns of trends in mean PDSI during 2000–2022 for (a) the full year, (b) the growing season and (c) the non-growing season. Green indicates wetting trends, and orange indicates drying trends. (d–f) Spatial distributions of drought categories based on mean PDSI for (d) the full year, (e) the growing season and (f) the non-growing season. Colors distinguish drought-free conditions, mild drought, moderate drought, severe drought and extremely drought.

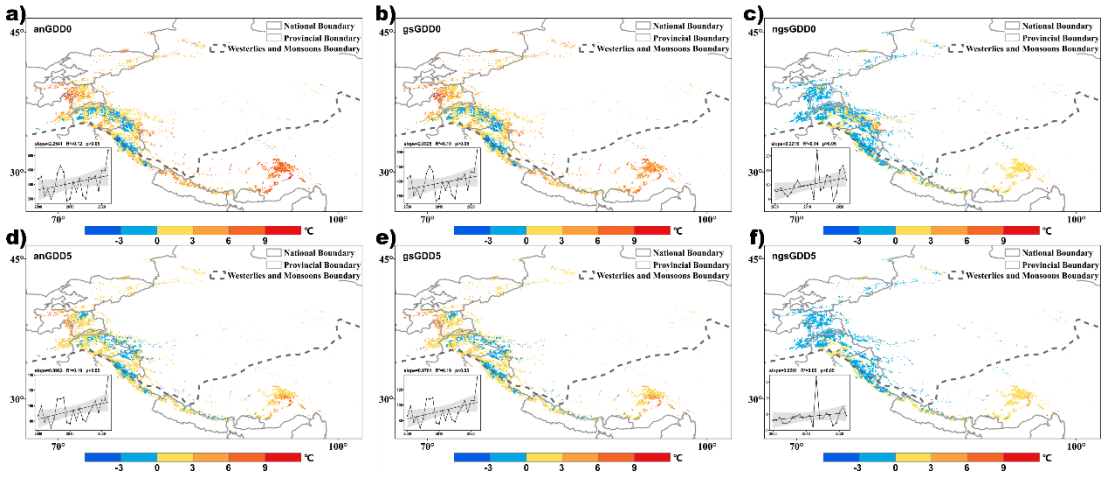


Figure S12. Spatial patterns of trends in growing degree days above 0 °C (GDD0) and 5 °C (GDD5) across glacier forefields of the Third Pole during 2000–2022.

(a–c) Trends in GDD0 for the full year, growing season and non-growing season, respectively. (d–f) Corresponding trends in GDD5. Colors indicate trend slopes, with positive values representing increasing heat accumulation and negative values representing decreasing heat accumulation. Insets in the lower left show interannual variation in the regional mean of each index and the fitted linear trend. Gray dashed lines mark the boundary between the westerly and monsoon regions.

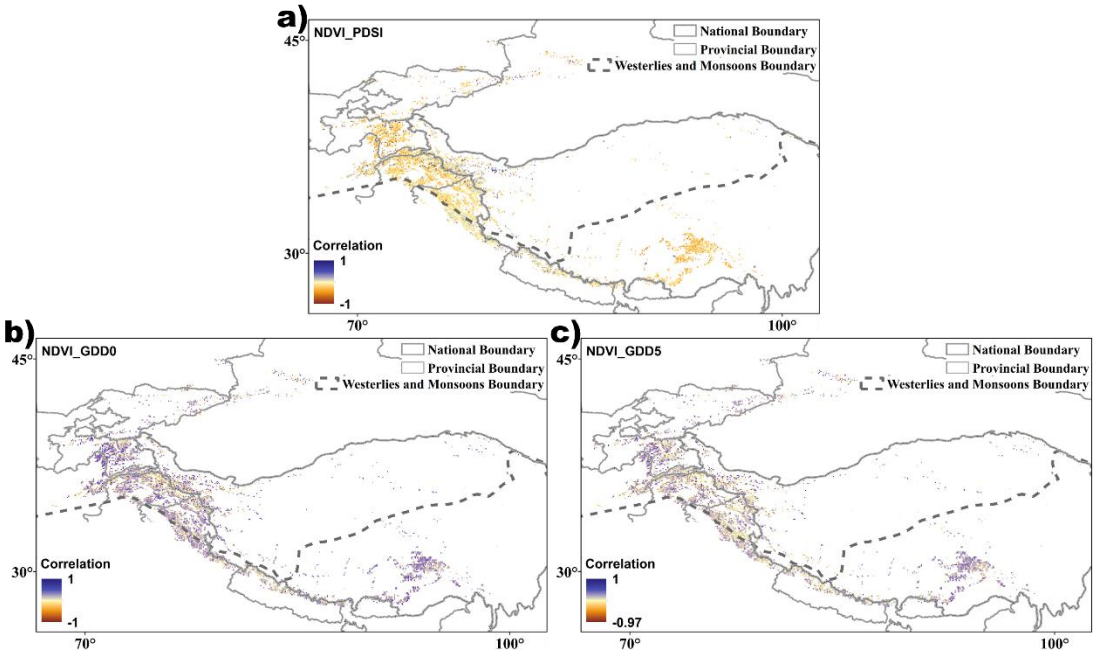


Figure S13. Spatial patterns of correlations between NDVI and PDSI, GDD0 and GDD5 across glacier forefields of the Third Pole.

Panels show correlation coefficients between NDVI and (a) PDSI, (b) GDD0 and (c) GDD5. Colors indicate correlation coefficients, with positive and negative values representing positive and negative correlations, respectively. Gray dashed lines mark the boundary between the westerly and monsoon regions.

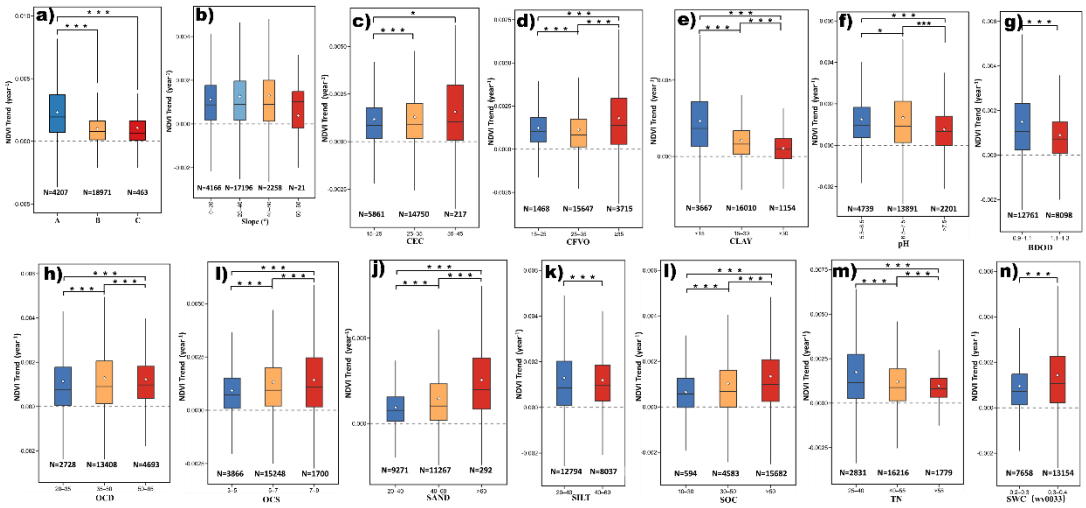


Figure S14. Variation in NDVI trends among deglaciation-age groups and environmental categories across glacier forefields of the Third Pole.

(a) Comparison of NDVI trends among deglaciation-age groups (group A, glacier retreat before 1990; group B, retreat during 1990–2006; and group C, retreat after 2006). (b) Variation among slope classes. (c–n) Variation among categories of soil properties. Boxes span the interquartile range, horizontal lines indicate medians, and points indicate means. The gray dashed line marks a trend slope of zero. Asterisks indicate statistical significance: *p < 0.05, **p < 0.01 and ***p < 0.001.

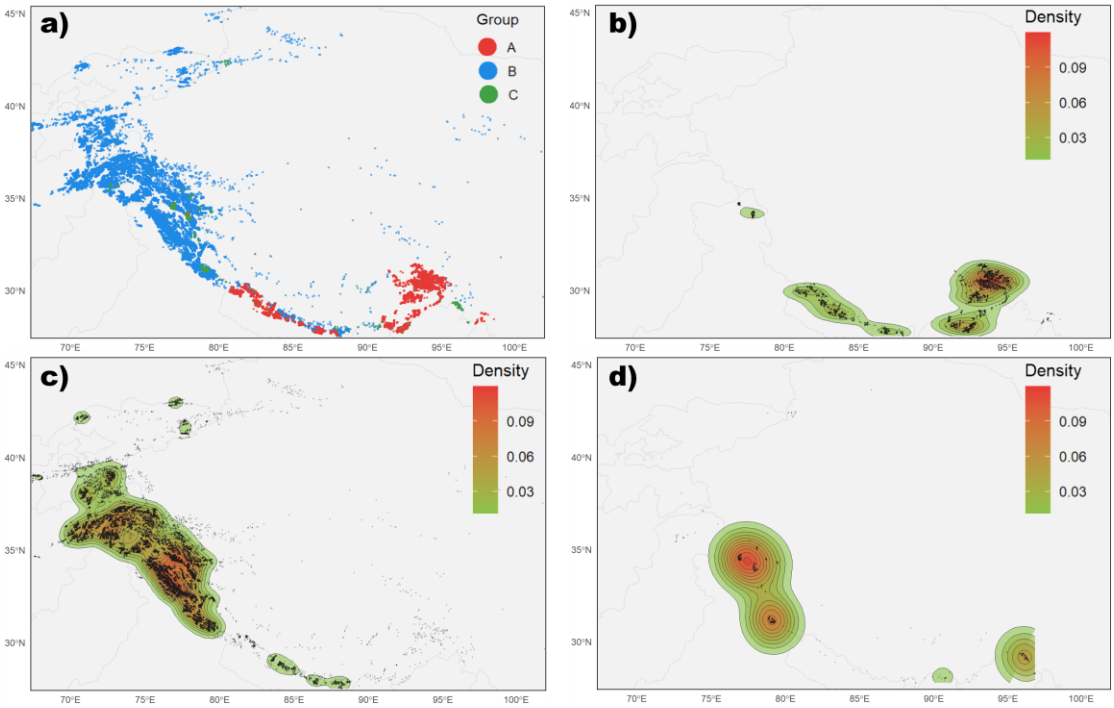


Figure S15. Spatial distribution of deglaciation-age groups across glacier forefields of the Third Pole.

(a) Spatial distribution of all sampling points classified into three groups according to the timing of glacier retreat: group A, before 1990; group B, 1990–2006; and group C, after 2006. These groups represent longer, intermediate and shorter periods since deglaciation, respectively. (b–d) Spatial kernel density distributions of sampling points in groups A, B and C, respectively.

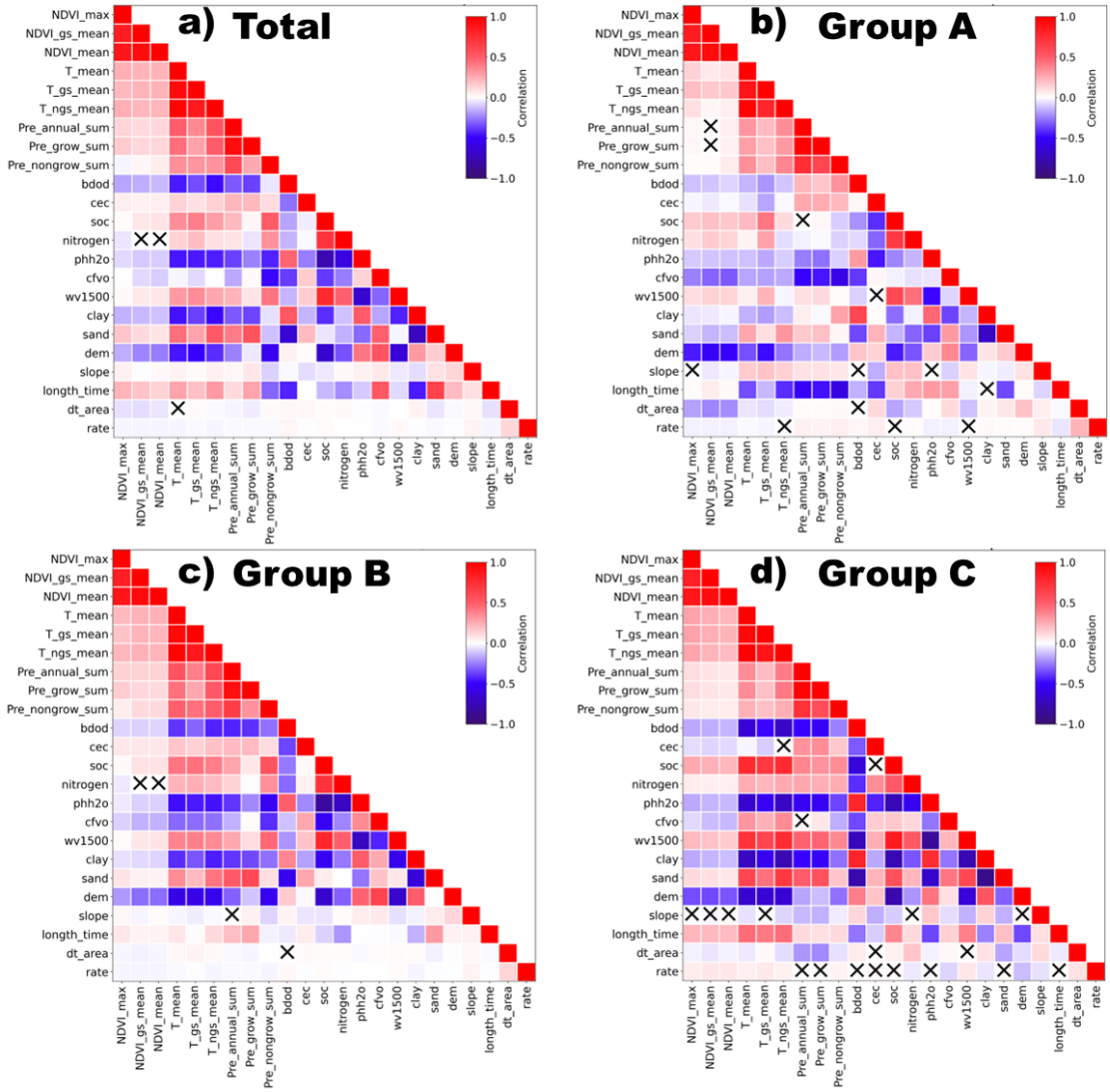


Figure S16. Correlation matrices of NDVI metrics and continuous environmental variables across glacier forefield deglaciation-age groups.

(a) All sampling points pooled across deglaciation-age groups. (b) Group A, deglaciated before 1990. (c) Group B, deglaciated during 1990–2006. (d) Group C, deglaciated after 2006. Crosses (×) mark correlations that are not statistically significant ($p \geq 0.05$). Colors indicate the direction and strength of correlations, with red denoting positive correlations and blue denoting negative correlations. Variables are ordered consistently across panels to facilitate comparison of correlation structures among deglaciation-age groups.